

**Scalar field self-force effects on orbits about a Schwarzschild black hole**Luz Maria Diaz-Rivera,<sup>1</sup> Eirini Messaritaki,<sup>1,2</sup> Bernard F. Whiting,<sup>1</sup> and Steven Detweiler<sup>1</sup><sup>1</sup>*Department of Physics, PO Box 118440, University of Florida, Gainesville, Florida 32611-8440, USA*<sup>2</sup>*Department of Physics, PO Box 413, University of Wisconsin-Milwaukee, Milwaukee, Wisconsin 53201, USA*

(Received 4 October 2004; published 16 December 2004)

For a particle of mass  $\mu$  and scalar charge  $q$ , we compute the effects of the scalar field self-force upon circular orbits, upon slightly eccentric orbits and upon the innermost stable circular orbit (ISCO) of a Schwarzschild black hole of mass  $m$ . For circular orbits the self-force is outward and causes the angular frequency at a given radius to decrease. For slightly eccentric orbits the self-force decreases the rate of the precession of the orbit. The effect of the self-force moves the radius of the innermost stable circular orbit inward by  $0.122\,701 \times q^2/\mu$ , and it increases the angular frequency of the ISCO by the fraction  $0.029\,165\,7 \times q^2/\mu m$ .

DOI: 10.1103/PhysRevD.70.124018

PACS numbers: 04.25.-g, 04.20.-q, 04.30.Db, 04.70.Bw

**I. INTRODUCTION**

We consider a small mass  $\mu$  with a scalar charge  $q$  which orbits a Schwarzschild black hole. The interaction of the particle with its own field yields the self-force on the particle. We use a perturbation analysis to find the effects of the scalar field self-force upon circular orbits, upon slightly eccentric orbits and upon the location of the innermost stable circular orbit (ISCO) of the Schwarzschild geometry. We view this project as a warm-up for the more interesting gravitational problem which must deal with more complicated field equations and gauge issues [1–3].

In general relativity, a particle of infinitesimal mass moves through spacetime along a geodesic. If the particle has a small but finite mass  $\mu$  then its world line deviates from a geodesic of the background spacetime by an amount proportional to  $\mu$ . This deviation is said to result from the “self-force” of the particle’s own gravitational field acting upon itself.

Newtonian gravity presents an elementary example of a self-force effect [4]. A small mass  $\mu$  in a circular orbit of radius  $r_o$  about a more massive companion  $m$  has an angular frequency  $\Omega_o$  given by

$$\Omega_o^2 = \frac{m}{r_o^3(1 + \mu/m)^2}. \quad (1)$$

When  $\mu$  is infinitesimal, the large mass  $m$  does not move, the radius of the orbit  $r_o$  is equal to the separation between the masses and  $\Omega_o^2 = m/r_o^3$ . However when  $\mu$  is finite but still small, both masses orbit their common center of mass with a separation of  $r_o(1 + \mu/m)$ , and the angular frequency is as given in Eq. (1). The finite  $\mu$  influences the motion of  $m$ , which influences the gravitational field within which  $\mu$  moves. This back action of  $\mu$  upon its own motion is the hallmark of a self-force, and the  $\mu$  dependence of Eq. (1) is properly described as a Newtonian self-force effect.

A thorough understanding of gravitational waves detected by the Laser Interferometer Space Antenna<sup>1</sup> will require clear theoretical predictions of possible gravitational wave forms which result from a small stellar-mass object orbiting a jumbo sized black hole; these wave forms must include self-force effects.

In studying the gravitational self-force, one considers the particle’s gravitational field to be a small perturbation  $h_{ab}$  of the background metric  $g_{ab}$ . For an object of very small size, the motion ought to be independent of the particle’s structure, and one is inclined to take the limit of a point particle. However, in that limit,  $h_{ab}$  diverges precisely at the particle, and the concept of the self-force might appear to be ill-defined.

Dirac [5] studied the electromagnetic version of this problem in flat spacetime and discovered that the part of the actual, retarded electromagnetic field which is singular and yet exerts no force on the particle itself is, in a local approximation, the Coulomb field and could be identified as the average of the retarded and advanced electromagnetic fields. The remainder, half of the difference between the retarded and advanced fields, is a vacuum solution of Maxwell’s equations and accounts entirely for the particle’s self-force.

The self-force includes the radiative reaction force or radiation reaction [6]. For a particle with electrical charge  $q$  and acceleration  $\vec{a}$ , the Abraham-Lorentz force describes the response of a particle to its own radiation and is proportional to  $q^2 d\vec{a}/dt$ . The factor of  $q^2$  results from the charge  $q$  interacting with its own electric field, which is also proportional to  $q$ . Similarly the gravitational radiation reaction force on a small mass  $\mu$  is proportional to  $\mu^2$ . Other parts of the self-force are not directly related to radiation but are properly described as the particle interacting with its own field and are also proportional to  $q^2$  or  $\mu^2$ .

<sup>1</sup>The LISA web site is located at <http://lisa.jpl.nasa.gov/>.

A curved-spacetime generalization of Dirac’s approach is now available [7–11]. For gravitation, an expansion about the position of the particle describes the singular “S” part of the field  $h_{ab}^S$  which exerts no force on the particle and is a local solution of the perturbed Einstein equations with the particle as the source. The remainder “R” part of the field  $h_{ab}^R = h_{ab} - h_{ab}^S$  is, locally, a source-free solution of the perturbed Einstein equations, with the combined metric  $g_{ab} + h_{ab}^R$  being a vacuum solution of the Einstein equations through first order in  $h_{ab}^R$ . The effect of the self-force has the particle moving along a geodesic of the vacuum geometry  $g_{ab} + h_{ab}^R$ .

A caveat remains: in curved-spacetime the S and R fields cannot be described in terms of the advanced and retarded fields. However, the mode-sum regularization procedure pioneered by Barack and Ori [12–21] is of use for background geometries amenable to the decomposition of fields in terms of scalar, vector, and tensor harmonics. This procedure has been applied to self-force calculations for the Schwarzschild geometry involving both scalar [19,22,23] and gravitational [24] fields. In general terms, the S field is singular at the particle, but each of its spherical harmonic components is finite; these components are the “regularization parameters.” The regular R field is determined by subtracting each  $\ell, m$  mode of the S field, from the corresponding  $\ell, m$  mode of the actual retarded field. The sum over modes of the difference between the retarded and S fields provides the R field which governs the self-force effects on the particle.

In this manuscript we treat the self-force from the scalar field  $\Psi$  in a perturbative manner. At zeroth order in  $\Psi$ , a geodesic for the particle is chosen and this determines the particle’s singular field  $\Psi^S$  in the neighborhood of the geodesic. Then the actual scalar field  $\Psi$ , with appropriate boundary conditions, is found everywhere. The difference of the actual field and the singular S field provides the regular remainder  $\Psi^R = \Psi - \Psi^S$ . Finally we determine the first order in  $\Psi$  self-force effects of the scalar field  $\Psi^R$  acting back on the particle and changing the world line away from the original geodesic. The small effects of  $\Psi^R$  appear as an acceleration of the world line of order  $q^2/\mu m^2$ . We determine the effects of the scalar field self-force upon the angular frequency, energy, and angular momentum of a general circular orbit, upon the rate of precession of a slightly eccentric orbit and upon the location and angular frequency of the innermost stable circular orbit.

In Sec. II we give an overview of the self-force and how it affects the location of the ISCO.

In Sec. III we describe how a generic scalar field affects the world line of a particle in the Schwarzschild geometry.

In Sec. IV we consider scalar field self-force effects on circular orbits, and numerically calculate the corresponding changes of energy, angular momentum, and angular frequency. In particular the self-force effect on the right-

hand side of Eq. (4), below, is derived. We also give the results of a numerical computation of  $\Psi^R$  evaluated at the location of the particle, which changes the effective inertial mass  $\mu$  of the particle.

In Sec. V we consider the scalar field self-force effects on slightly eccentric orbits of the Schwarzschild geometry. Specifically, we find the self-force correction to the rate of the precession of the orbit and to the right-hand side of Eq. (5), below. In Sec. VI, this analysis is applied to an orbit near  $r = 6m$  to obtain the self-force effect upon the radius and angular frequency of the ISCO.

The discussion of Sec. VII distinguishes between the scalar and gravitational self-force effects. We do not attempt to generalize our limited results to the case of the gravitational self-force.

In Appendix A we give some details of the spherical harmonic decomposition of a source moving along a slightly eccentric orbit. These details are required for the numerical calculation of the actual field for a slightly eccentric orbit.

In Appendix B we describe the regularization parameters which are required for the self-force analysis of slightly eccentric circular orbits of the Schwarzschild geometry. These are used in the computation of  $\Psi^R$  described in Secs. IV, V, and VI.

We use Schwarzschild coordinates  $(t, r, \theta, \phi)$  on the spacetime manifold. The position of the particle in these coordinates is  $(T, R, \Theta, \Phi)$ , and  $s$  measures the proper time along a world line. For a general world line, the angular frequency is  $\Omega_\phi \equiv d\Phi/dT$ . The subscript  $o$  is reserved exclusively for quantities related to circular orbits: for a circular orbit, the radius and angular frequency are  $r_o$  and  $\Omega_o$ , respectively, while  $\Psi_o$  is the scalar field from a particle in a circular orbit. The mass and charge of a particle are  $\mu$  and  $q$ , and the mass of the black hole is  $m$ . The scalar field is  $\Psi$ ; however, we define  $\psi \equiv q\Psi/\mu$  as a combination which occurs often in the description of the effects of a scalar field on the motion of a particle. In this perturbative analysis we always assume that  $q^2/\mu \ll m$ .

In equations concerning the self-force, expressions containing  $\psi$  refer to the regularized field and must be evaluated at the location of the particle.

## II. CONCEPTUAL FRAMEWORK

### A. Dissipative and conservative forces

Mino [25] examines the self-force on a particle in orbit about a rotating black hole with a focus on how the Carter constant [26] evolves. Following Mino’s ideas, one is naturally led to divide the self-force into two parts which depends upon how each part changes under a change in the boundary conditions. One part is “dissipative” and usually associated with radiation reaction. The other part is “conservative.” This distinction is most easily described in terms of “Green’s functions” which yield the parts of the

field responsible for the dissipative and conservative parts of the self-force.

Let  $G^{\text{ret}}$  be the retarded Green's function, which provides the actual, physical field  $\Psi^{\text{ret}}$  for the problem of interest, and let  $G^{\text{S}}$  be the Green's function [10] for the singular part of the field  $\Psi^{\text{S}}$ . The regularized field  $\Psi^{\text{R}} = \Psi^{\text{ret}} - \Psi^{\text{S}}$  provides the complete self-force. The change in boundary conditions from outgoing radiation at infinity to incoming radiation is effected by using the advanced Green's function  $G^{\text{adv}}$  and its field  $\Psi^{\text{adv}}$ , rather than the retarded quantities.

The dissipative part of the self-force changes sign under the interchange of the retarded and advanced Green's functions. Thus, the dissipative part of the field  $\Psi^{\text{dis}}$  is uniquely determined by using a "Green's function"

$$G^{\text{dis}} = \frac{1}{2}G^{\text{ret}} - \frac{1}{2}G^{\text{adv}}. \quad (2)$$

$\Psi^{\text{dis}}$  is a source-free solution of the field equation and is regular at the particle; no use of  $\Psi^{\text{S}}$  is required to find the dissipative part of the self-force.

The conservative part of the self-force is invariant under the interchange of the retarded and advanced Green's functions. The conservative part of the field represents the half-advanced plus half-retarded field, but this is singular at the particle and requires regularization by the removal of  $\Psi^{\text{S}}$ . Thus, the conservative part of the regularized field is uniquely determined near the particle by using a "Green's function"

$$G^{\text{con}} = \frac{1}{2}G^{\text{ret}} + \frac{1}{2}G^{\text{adv}} - G^{\text{S}}. \quad (3)$$

In a neighborhood of the particle, the resulting field is a source-free solution of the field equation and is regular.

A circular orbit about a Schwarzschild black hole provides an example which clearly distinguishes the dissipative from the conservative parts of the self-force. For a particle in a circular orbit about a black hole,  $\partial_t\Psi$  and  $\partial_\phi\Psi$  are both dissipative, as can be understood in terms of time-reversal invariance. We see below in Eqs. (16) and (17) that  $\partial_t\Psi$  and  $\partial_\phi\Psi$  are responsible for removing energy and angular momentum, respectively, from the particle at a rate which precisely balances the loss of energy and angular momentum outward through a distant boundary and into the black hole. With  $t \rightarrow -t$  and  $\phi \rightarrow -\phi$  the motion of the particle is nearly identical, only the boundary conditions on the scalar field are changed, and now energy and angular momentum entering the system through the boundary are deposited on the particle. The dissipative self-force is small in this perturbative analysis but its effect accumulates over time as the particle spirals slowly inward or outward, depending upon the boundary conditions.

For a circular orbit  $\partial_r\Psi$  is conservative and, as shown below, provides a small addition to the centripetal force which affects the angular frequency via a change in the

right-hand side of Eq. (4). However, the angular frequency is unchanged under  $t \rightarrow -t$  and  $\phi \rightarrow -\phi$  which changes the direction of radiation flow at the boundary.  $\partial_r\Psi$  and its effect on the angular frequency is independent of the direction of radiation imposed by the boundary conditions. With either boundary condition the conservative self-force effect on the frequency is small but the effect on the phase of the orbit accumulates over time.

If a particle is not in a circular orbit, then these simple relationships between the components of  $\partial_a\Psi$  and the conservative and dissipative parts of the self-force no longer hold.

## B. Stability of a circular orbit

The notion of the stability of a circular orbit in the context of the self-force warrants further discussion.

A stability problem presupposes the existence of a mechanical system in equilibrium. A perturbation analysis of the system's small oscillations often reveals that the natural frequencies of the system are complex eigenvalues dependent upon some set of parameters. The sign of the imaginary part of a natural frequency determines whether the amplitude of a small oscillation grows, diminishes, or stays constant. The simplest cases are when the frequency is either purely real or purely imaginary. An imaginary frequency with an appropriate sign then signifies an unstable mode.

For the system of a small particle of mass  $\mu$  orbiting a larger black hole of mass  $m$ , the particle moves along a geodesic, if  $\mu$  is considered infinitesimal. In this case it is well-known that for a circular orbit at Schwarzschild coordinate  $r = r_o$  the angular frequency  $\Omega_o$ , with respect to Schwarzschild coordinate time, is given by

$$\Omega_o^2 = \frac{m}{r_o^3}. \quad (4)$$

If the orbit has a small eccentricity then elementary analysis [27] reveals that the frequency  $\Omega_r$  of the radial oscillations is determined by

$$\Omega_r^2 = \frac{m}{r_o^4}(r_o - 6m). \quad (5)$$

If  $r_o$  is very large, then  $\Omega_o$  and  $\Omega_r$  are nearly equal, and the slightly eccentric orbit is an ellipse obeying Kepler's laws. The difference between  $\Omega_o$  and  $\Omega_r$  leads to the rate of the precession of the ellipse,

$$\Omega_{\text{pr}} = \Omega_o - \Omega_r, \quad (6)$$

and is directly responsible for the relativistic contribution to the precession of the perihelion of Mercury. For an orbit just inside  $6m$ , the two solutions for  $\Omega_r$  in Eq. (5) are both imaginary and one corresponds to an unstable mode. The orbit at  $r_o = 6m$  is the innermost stable circular orbit—the ISCO.

For realistic boundary conditions, the expectation is that at a large separation the emission of gravitational radiation from a binary circularizes the orbit [28] and causes the two objects to spiral slowly towards each other.

When  $r_o$  is outside but comparable to  $6m$ , gravitational radiation evolves the orbit slowly inward on a secular time scale  $m/\mu$  times longer than the dynamical time scale, with the rate of inspiral  $dr_o/dt = O(\mu/m)$ . The particle makes a transition to a plunge [29] when it reaches the ISCO, and the plunge occurs over a dynamical time scale. The resulting gravitational wave form appears as a sinusoid with a slowly increasing frequency until the angular frequency of the ISCO is reached. Then, after a brief burst from the plunge, the wave form is determined by the frequencies of the most weakly damped free oscillations of the black hole [30–32].

The secular evolution caused by gravitational radiation keeps the particle from ever being in true equilibrium, and the question of the stability of a circular orbit may seem ill-posed. Nevertheless, the gravitational wave form changes character at a frequency near that in Eq. (4) for  $r_o = 6m$  even though the particle is never actually in equilibrium. The dependence of the transition frequency upon the scalar field self-force is a major focus of this manuscript.

To form a well-posed problem related to the ISCO and the angular frequency of the transition to a plunge, we consider an unphysical system with boundary conditions which have equal amounts of outgoing and incoming radiation. Such a system must be constructed by use of a regularized half-advanced and half-retarded Green's function. In this case, the dissipative force vanishes entirely while the conservative force and its effects upon  $\Omega_o$  and  $\Omega_r$  are unchanged from the case with realistic outgoing-wave boundary conditions. With equal amounts of outgoing and incoming radiation, equilibrium configurations exist, and stability analyses may proceed.

In Sec. V we show that the conservative force from  $\nabla_a \Psi$  changes the right-hand side of Eq. (5), and therefore the location of the actual ISCO by a fractional amount of order  $q^2/\mu m$  for a scalar field; for gravity this fractional amount would be of order  $\mu/m$ .

### III. SCALAR FIELD EFFECTS ON A PARTICLE'S MOTION

#### A. Description of motion

The functions  $[T(s), R(s), \pi/2, \Phi(s)]$  describe a particle's world line in the equatorial plane of a black hole in Schwarzschild coordinates  $(t, r, \theta, \phi)$ . The proper time  $s$  is measured along the world line, and the four-velocity

$$u^a = dx^a/ds \quad (7)$$

is normalized to unity,  $u^a u_a = -1$ . Additionally, the world line and the Killing vector fields  $t^a \partial/\partial x^a \equiv \partial/\partial t$  and  $\phi^a \partial/\partial x^a \equiv \partial/\partial \phi$  define

$$E \equiv -t^a u_a \quad \text{and} \quad J \equiv \phi^a u_a, \quad (8)$$

which, for geodesic motion, are the energy and angular momentum, per unit rest mass, respectively. The components of  $u^a$  are thus

$$u^a = \left( \frac{E}{1 - 2m/R}, \dot{R}, 0, J/R^2 \right), \quad (9)$$

where the dot denotes a derivative with respect to  $s$ . For any world line the angular frequency, with respect to Schwarzschild coordinate time, is

$$\Omega_\phi \equiv \dot{\Phi}/\dot{T} = \frac{d\Phi}{dT} = \frac{J(R - 2m)}{ER^3}. \quad (10)$$

The normalization of  $u^a$  implies that

$$u^a u_a = -1 = -\frac{(E^2 - \dot{R}^2)}{1 - 2m/R} + \frac{J^2}{R^2} \quad (11)$$

or

$$E^2 - \dot{R}^2 = (1 - 2m/R)(1 + J^2/R^2). \quad (12)$$

#### B. Scalar field modifications of the geodesic equation

Quinn [33] considers the interaction of a scalar field  $\Psi$  with a particle of constant bare mass  $\mu_0$  and constant scalar charge  $q$ . He carefully demonstrates that the equation of motion is

$$u^b \nabla_b (\mu u_a) = \dot{\mu} u_a + \mu u^b \nabla_b u_a = q \nabla_a \Psi, \quad (13)$$

where  $\mu = \mu_0 - q\Psi$ . This result can be obtained from a general action principle. In what follows,  $\Psi$  is assumed to be the regular field  $\Psi^R$  evaluated at the particle. Thus, the quantity  $\mu$  changes when the value of the scalar field at the particle changes. The fractional change in  $\mu$  is

$$\Delta\mu/\mu_0 = -q\Psi/\mu_0, \quad (14)$$

which is shown in Figs. 1 and 2 for circular orbits of the Schwarzschild geometry.

The projection of Eq. (13) orthogonal to  $u^a$  yields the acceleration from the self-force

$$u^b \nabla_b u_a = (q/\mu)(g_a^b + u_a u^b) \nabla_b \Psi \quad (15)$$

which modifies the world line of the particle through spacetime. In our perturbative analysis, we only consider the first order effects of the scalar field. The right-hand side of Eq. (15) is explicitly first order in  $\Psi$ , and the change in  $\mu$  has only a second order effect on the acceleration. Thus, for the purposes of describing the world line of the particle we treat  $\mu$  as constant, and it is convenient to define  $\psi \equiv q\Psi/\mu$ . For simplicity we also assume that the scalar field is symmetric under reflection through the equatorial plane and that the particle remains in the equatorial plane.

The components of Eq. (15) yield

$$dE/ds = \dot{E} = -\partial_t \psi + E u^b \nabla_b \psi \quad (16)$$

$$dJ/ds = \dot{J} = \partial_\phi \psi + Ju^b \nabla_b \psi \quad (17)$$

and

$$\begin{aligned} \ddot{R} = & -\frac{m(E^2 - \dot{R}^2)}{R(R-2m)} + \frac{R-2m}{R^4} J^2 + \frac{R-2m}{R} \partial_r \psi \\ & + \dot{R} u^b \nabla_b \psi. \end{aligned} \quad (18)$$

The normalization (12) is a first integral of the equation of motion, and Eq. (18) follows directly from Eqs. (12), (16), and (17), which form a complete set of equations describing the equatorial motion of a particle interacting with a scalar field.

Together, Eqs. (12) and (18) imply that

$$\ddot{R} = -\frac{m}{R^2} + \frac{R-3m}{R^4} J^2 + \frac{R-2m}{R} \partial_r \psi + \dot{R} u^b \nabla_b \psi, \quad (19)$$

which is convenient for analyzing slightly eccentric orbits.

For a particle in circular motion,  $\partial_r \psi$  is independent of the direction of radiation at the boundaries and provides a conservative force. However,  $\partial_t \psi$  and  $\partial_\phi \psi$  on the right-hand sides of Eqs. (16) and (17) are dissipative components of the self-force and change sign if the direction of radiation at the boundary is changed. In fact, the conservation of energy and angular momentum guarantee that Eqs. (16) and (17) are consistent with the flow of energy and angular momentum across the boundaries. This is manifest by matching appropriate independent solutions of the source-free wave equation at the orbit of the particle. If a particle is not in a circular orbit, then these simple relationships between the components of  $\partial_a \psi$  and the conservative and dissipative parts of the self-force no longer hold.

#### IV. SELF-FORCE EFFECTS ON CIRCULAR ORBITS

The scalar field  $\psi_o$  of a charged particle in a circular orbit rotates with the particle and has a symmetry described by

$$\partial_t \psi_o + \Omega_o \partial_\phi \psi_o = 0. \quad (20)$$

In particular, this implies that  $u^a \nabla_a \psi_o = 0$  at the particle and simplifies the description of the self-force for circular motion. A world line is ‘‘instantaneously circular’’ at radius  $r_o$  if  $\dot{R} = \ddot{R} = 0$ . In this case

$$J^2 = \frac{r_o^4}{r_o - 3m} \left( \frac{m}{r_o^2} - \frac{r_o - 2m}{r_o} \partial_r \psi_o \right) \quad (21)$$

follows from Eq. (19), and

$$E^2 = \frac{(r_o - 2m)^2}{r_o(r_o - 3m)} (1 - r_o \partial_r \psi_o) \quad (22)$$

then follows from Eq. (12). The angular frequency is given by Eq. (10)

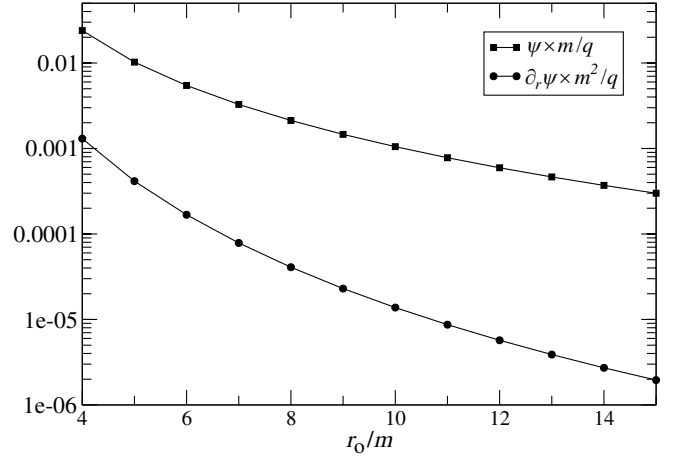


FIG. 1. The regularized field  $\Psi_o^R m/q$  at the particle and the radial component of the self-force  $(\partial_r \Psi_o^R) m^2/q$  as a function of the radius  $r_o$  for circular orbits close to the black hole.

$$\Omega_o^2 = \frac{m}{r_o^3} - \frac{r_o - 3m}{r_o^2} \partial_r \psi_o + O(\psi^2). \quad (23)$$

These reduce to the usual expressions for the circular geodesics of the Schwarzschild geometry when the scalar field  $\psi_o$  is removed. The resulting fractional changes in  $J$ ,  $E$ , and  $\Omega_o$  caused by the self-force for an orbit at radius  $r_o$  are

$$\frac{\Delta J}{J} = -\frac{r_o(r_o - 2m)}{2m} \partial_r \psi_o, \quad (24)$$

$$\frac{\Delta E}{E} = -\frac{1}{2} r_o \partial_r \psi_o, \quad (25)$$

and

$$\frac{\Delta \Omega_o}{\Omega_o} = -\frac{r_o(r_o - 3m)}{2m} \partial_r \psi_o. \quad (26)$$

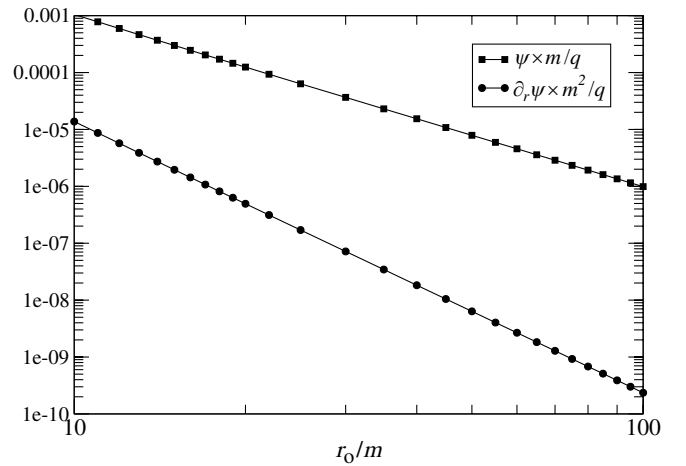


FIG. 2. The same as Fig. 1 except for larger radii.

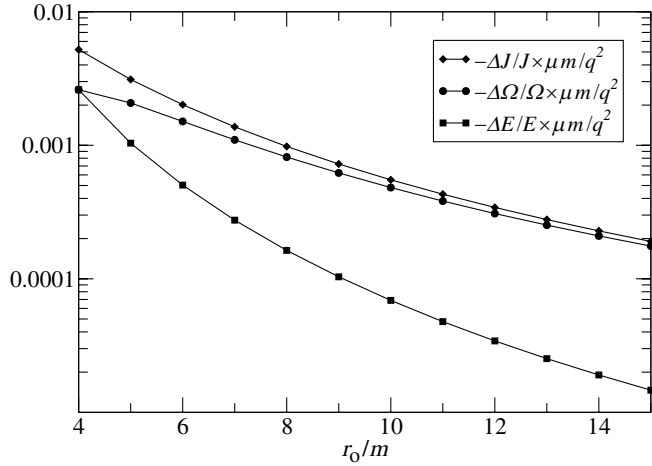


FIG. 3. The fractional changes in  $J$ ,  $E$ , and  $\Omega_o$ , from the self-force as a function of the radius  $r_o$  for circular orbits close to the black hole. These quantities are calculated using Eqs. (24)–(26).

References [19,23,34] give detailed descriptions of the calculation of the retarded scalar field for a particle in a circular orbit of the Schwarzschild geometry. References [12,15,17–21] describe the evaluation of the required regularization parameters for the self-force. In Appendix B, we give the regularization parameters for the scalar field  $\psi^R$  from Ref. [20]. References [19,23] describe implementations of the Barack and Ori regularization procedure for the numerical evaluation of the self-force for circular orbits of the Schwarzschild geometry.

Figures 1 and 2 show the regularized  $\psi^R$  and the radial component of the self-force  $\partial_r \psi^R$  evaluated at the particle as functions of the radius of the orbit. Figures 3 and 4 show the fractional changes in  $J$ ,  $E$ , and  $\Omega_o$  from the radial component of the self-force. Table I gives a selection of our numerical calculations of both  $\psi^R$  and  $\partial_r \psi^R$  at the particle as a function of  $R$ . The force is outward, falls off approximately as  $r_o^{-5}$ , as noted by Burko [23], and  $\psi^R$  falls

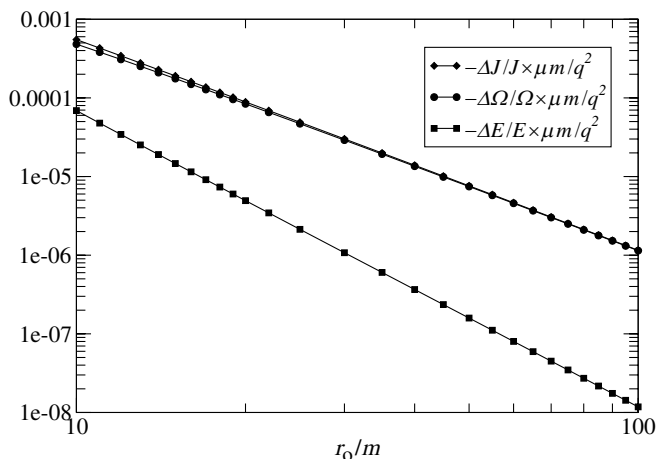


FIG. 4. The same as Fig. 3 except for larger radii.

off as  $r_o^{-3}$  for large  $r_o$ . Each of  $\Omega_o$ ,  $E$ , and  $J$  for a circular orbit is decreased by the self-force.

A very interesting analysis of Hikida *et al.* [35,36] uses a novel decomposition of  $\Psi$  into singular and regular parts. Post-Newtonian analysis, at 18PN order, on their singular part and evaluation of their regular part up to  $\ell = 19$  yield results for  $\partial_r \Psi_o^R$  which agree well with ours given in Table I. The relative difference is  $10^{-7}$ , except near  $r_o = 6m$  where the difference is  $10^{-4}$ .

## V. SELF-FORCE EFFECTS ON SLIGHTLY ECCENTRIC ORBITS

A particle in an orbit with small eccentricity, in the Schwarzschild geometry, has periodic motion in the radial direction with a frequency  $\Omega_r$  given in Eq. (5). In this section we describe the effects of the self-force on  $\Omega_r$  and upon the rate of precession of the orbit  $\Omega_{pr}$ . We require that the scalar field  $\psi$  have boundary conditions with equal amplitudes of incoming and outgoing radiation at both the event horizon and infinity. This simplifies the discussion of  $\Omega_r$  and allows us to pose a well-defined stability problem for the ISCO. The conservative ‘‘Green’s function’’  $G^{\text{con}}$  determines the regularized field.

### A. Slightly eccentric geodesics

In this perturbative analysis, a slightly eccentric geodesic about a fixed radius  $r_o$  with a small amplitude,  $\delta R \ll q^2/\mu \ll r_o q^2/\mu^2 \ll r_o$ , is described by

$$R[T(s)] = r_o + \delta R \cos[\Omega_r T(s)] \quad (27)$$

and

$$\Phi(T) = \Omega_o T + \frac{d\Omega_\phi}{dR} \frac{\delta R}{\Omega_r} \sin(\Omega_r T). \quad (28)$$

The remainder of the analysis treats  $\delta R$  as a small quantity, and only terms through first order in  $\delta R$  are retained. The angular frequency of this geodesic orbit is a function of time,

$$\Omega_\phi \equiv \frac{d\Phi}{dT} = \Omega_o + \frac{d\Omega_\phi}{dR} \delta R \cos(\Omega_r T). \quad (29)$$

The frequencies  $\Omega_o$  and  $\Omega_r$  are given in Eqs. (4) and (5). The quantity  $d\Omega_\phi/dR$  represents the change in angular frequency, from Eq. (10), with respect to a change in radius while  $E$  and  $J$  are held constant,

$$\frac{d\Omega_\phi}{dR} = -\frac{2(R-3m)}{R(R-2m)} \Omega_\phi. \quad (30)$$

The radial velocity is

$$\frac{dR}{dT} = -\Omega_r \delta R \sin(\Omega_r T). \quad (31)$$

TABLE I. A selection of our computed values of the regularized scalar field evaluated at the particle and the radial component of the self-force, for circular orbits of radius  $r_o$ . Also shown are  $F_r$ ,  $F_t$ , and  $F_\phi$ , defined in Eqs. (33)–(35), for slightly eccentric orbits with  $r_o > 6m$ ; for  $r_o = 6m$ , their limiting values are given; for  $r_o < 6m$  slightly eccentric orbits do not exist and  $F_r$ ,  $F_t$ , and  $F_\phi$  are not defined.

$r_o/m$	$\Psi_o^R m/q$	$\partial_r \Psi_o^R m^2/q$	$F_r \mu m^3/q^2$	$F_t \mu m^2/q^2$	$F_\phi \mu m/q^2$
4	-0.023 987 75	0.001 302 375			
5	-0.010 234 18	$4.149 937 \times 10^{-4}$			
6	-0.005 454 828	$1.677 283 4 \times 10^{-4}$	$-1.381 375 6 \times 10^{-4}$	0.004 923 88	-0.028 221 7
7	-0.003 275 343	$7.850 679 \times 10^{-5}$	$-6.108 26 \times 10^{-5}$	0.002 459 81	-0.017 533 1
8	-0.002 127 506	$4.082 502 \times 10^{-5}$	$-2.916 65 \times 10^{-5}$	0.001 355 06	-0.011 899 1
10	-0.001 049 793	$1.378 448 \times 10^{-5}$	$-8.216 72 \times 10^{-6}$	$5.076 81 \times 10^{-4}$	-0.006 420 25
14	$-3.700 646 \times 10^{-4}$	$2.720 083 \times 10^{-6}$	$-1.192 80 \times 10^{-6}$	$1.196 75 \times 10^{-4}$	-0.002 640 01
20	$-1.246 728 \times 10^{-4}$	$4.937 906 \times 10^{-7}$	$-1.552 96 \times 10^{-7}$	$2.687 98 \times 10^{-5}$	-0.001 059 72
30	$-3.661 710 \times 10^{-5}$	$7.171 924 \times 10^{-8}$	$-1.549 04 \times 10^{-8}$	$5.089 27 \times 10^{-6}$	$-3.824 35 \times 10^{-4}$
50	$-7.889 518 \times 10^{-6}$	$6.346 791 \times 10^{-9}$	$-8.535 32 \times 10^{-10}$	$6.444 98 \times 10^{-7}$	$-1.072 42 \times 10^{-4}$
70	$-2.877 222 \times 10^{-6}$	$1.284 529 \times 10^{-9}$	$-1.260 87 \times 10^{-10}$	$1.669 32 \times 10^{-7}$	$-4.654 96 \times 10^{-5}$
100	$-9.884 245 \times 10^{-7}$	$2.356 504 \times 10^{-10}$	$-1.651 35 \times 10^{-11}$	$4.005 31 \times 10^{-8}$	$-1.922 77 \times 10^{-5}$
200	$-1.239 866 \times 10^{-7}$	$8.642 538 \times 10^{-12}$	$-3.117 90 \times 10^{-13}$	$2.514 66 \times 10^{-9}$	$-3.444 12 \times 10^{-6}$

### B. Self-force effect upon $J$ for slightly eccentric orbits

For slightly eccentric orbits, with self-force effects included,  $J$  is not a constant of the motion, even with no dissipation. The effect of the self-force on  $J$  is given in Eq. (17),

$$dJ/ds = \partial_\phi \psi + Ju^a \nabla_a \psi \quad \text{or}$$

$$dJ/dT = (u^t)^{-1} \partial_\phi \psi + J(\partial_t + \Omega_\phi \partial_\phi) \psi + J \frac{dR}{dT} \partial_r \psi. \quad (32)$$

The  $\psi$  for a slightly eccentric orbit is described in Appendix A. We note here that it has two parts. The larger part  $\psi_o$  is equal to the field which would result from pure circular motion at  $r_o$  and consists of frequencies which are integral multiples of  $\Omega_o$ . For a circular orbit, in general,  $(\partial_t + \Omega_o \partial_\phi) \psi_o = 0$ , and with conservative boundary conditions  $\partial_t \psi_o = \partial_\phi \psi_o = 0$  at the particle. The smaller part is proportional to  $\delta R$ . In Appendix A we show that for slightly eccentric orbits an expansion for  $\psi$  around a circular orbit at  $r_o$  gives

$$\partial_t \psi = -F_t \Omega_r \delta R \sin(\Omega_r T), \quad (33)$$

$$\partial_\phi \psi = -F_\phi \Omega_r \delta R \sin(\Omega_r T), \quad (34)$$

and

$$\partial_r \psi = [\partial_r \psi_o]_{r_o} + F_r \delta R \cos(\Omega_r T), \quad (35)$$

where  $F_t$ ,  $F_\phi$ , and  $F_r$  depend only upon  $r_o$  and, are independent of both  $\delta R$  and  $t$ . In this section the subscript  $r_o$  on  $[\partial_r \psi_o]_{r_o}$  implies that  $\partial_r \psi_o$  is to be evaluated at the circular orbit  $r_o$  and not at the actual location of the particle. In Eq. (32) the coefficient of  $\partial_r \psi$  is already first order in  $\delta R$ , and it is sufficient to use only the circular orbit value  $[\partial_r \psi_o]_{r_o}$  at the particle. Thus,

$$\frac{dJ}{dR} = \frac{dJ}{dT} \left( \frac{dT}{dR} \right)^{-1} = JF_t + EF_\phi + J[\partial_r \psi_o]_{r_o}, \quad (36)$$

where we have used Eqs. (31), (33), and (34), along with Eqs. (9)–(12).

### C. Self-force effects upon $\Omega_r$ for slightly eccentric orbits

The exact radial equation of motion (19), which includes the self-force, is

$$\ddot{R} = -\frac{m}{R^2} + \frac{R-3m}{R^4} J^2 + \frac{R-2m}{R} \partial_r \psi + \dot{R} u^b \nabla_b \psi. \quad (37)$$

For describing slightly eccentric orbits, we expand this equation around the circular orbit at  $r_o$  by letting  $R \rightarrow r_o + \delta R \cos(\Omega_r T)$  and dropping all terms of order  $\delta R^2$ . The  $O(\delta R^0)$  part is equivalent to Eq. (21) for the circular orbit value of  $J^2$ . The  $\dot{R} u^b \nabla_b \psi$  term is  $O(\delta R^2)$ . The part of Eq. (37) which is first order in  $\delta R$  is

$$\ddot{R} = \frac{d}{dR} \left[ -\frac{m}{R^2} + \frac{R-3m}{R^4} J^2 + \frac{R-2m}{R} \partial_r \psi \right]_{r_o} \delta R \cos(\Omega_r T). \quad (38)$$

After use of Eq. (35), which gives  $d(\partial_r \psi)/dR = F_r$ , this becomes

$$\ddot{R} = \left[ -\frac{m(r_o-6m)}{r_o^3(r_o-3m)} + \frac{3(r_o-4m)(r_o-2m)}{r_o^2(r_o-3m)} (\partial_r \psi_o)_{r_o} + \frac{2m}{r_o^2} (\partial_r \psi_o)_{r_o} + \frac{(r_o-3m)}{r_o^4} \frac{dJ^2}{dR} + \frac{(r_o-2m)}{r_o} F_r \right] \delta R \cos(\Omega_r T). \quad (39)$$

Equation (27) implies that

$$\ddot{R} = -\frac{\Omega_r^2 E^2 \delta R \cos(\Omega_r T)}{(1 - 2m/r_o)^2}. \quad (40)$$

Using Eq. (22) for  $E^2$ , we finally obtain

$$\begin{aligned} \Omega_r^2 = & \frac{m}{r_o^4}(r_o - 6m) - \frac{2J}{r_o^5}(r_o - 3m)^2(JF_t + EF_\phi) \\ & - \frac{1}{r_o^3}(r_o - 2m)(r_o - 3m)(3[\partial_r \psi_o]_{r_o} + rF_r) \end{aligned} \quad (41)$$

through first order in  $\psi$ . This provides the scalar field self-force correction to Eq. (5) for  $\Omega_r^2$ .

To examine the effect of the self-force on  $\Omega_r$  for  $r_o \approx 6m$ , let  $f$  represent all but the first term on the right-hand side of Eq. (41). The change in  $\Omega_r^2$  caused by the self-force is then

$$\Delta(\Omega_r^2) = f = f_0 + f_1(r_o - 6m) + \dots \quad (42)$$

Numerical analysis determines the values  $f_0 = 9.467\,68 \times 10^{-5} q^2/\mu m^3$ , and  $f_1 = -3.2318 \times 10^{-5} q^2/\mu m^2$ . For  $r_o = 6m$ ,

$$\Delta\Omega_r \Big|_{r_o \rightarrow 6m} = f_0^{1/2} = 9.730\,20 \times 10^{-3} q/\mu^{1/2} m^{3/2}. \quad (43)$$

More generally, the change in  $\Omega_r$  caused by the self-force is

$$\Delta\Omega_r = \left[ \frac{m}{r_o^4}(r_o - 6m) + f \right]^{1/2} - \left[ \frac{m}{r_o^4}(r_o - 6m) \right]^{1/2}. \quad (44)$$

When  $r_o$  increases away from  $6m$ ,  $\Delta\Omega_r$  decreases and changes scale

$$\text{for } r_o - 6m \gg q^2/\mu,$$

$$\Delta\Omega_r \approx \frac{f r_o^2}{2} [m(r_o - 6m)]^{-1/2} = O(q^2/\mu m^2). \quad (45)$$

The numerical calculation of  $\Delta\Omega_r$ , based upon Eq. (45), is presented in Figs. 5 and 6. Figure 5 illustrates the small end of this range, where  $q^2/\mu \ll r_o - 6m \ll m$  and  $f \approx f_0$ . In this case,

$$\Delta\Omega_r \approx 6.957\,30 \times 10^{-4} (r_o/6m - 1)^{-1/2} q^2/\mu m^2 \quad (46)$$

gives the limit of the curve in Fig. 5 as  $r_o$  approaches  $6m$ . The right-hand sides of Eqs. (43) and (46) are equal at

$$\frac{r_o}{6m} - 1 \approx \frac{r_o^4}{24m^2} f_0 = 0.005\,112\,55 q^2/\mu m. \quad (47)$$

At larger separations  $r_o - 6m \gtrsim m$ ,  $\Delta\Omega_r$  is still approximated by Eq. (45) and scales as  $1/r_o^2$  as illustrated in Fig. 6.

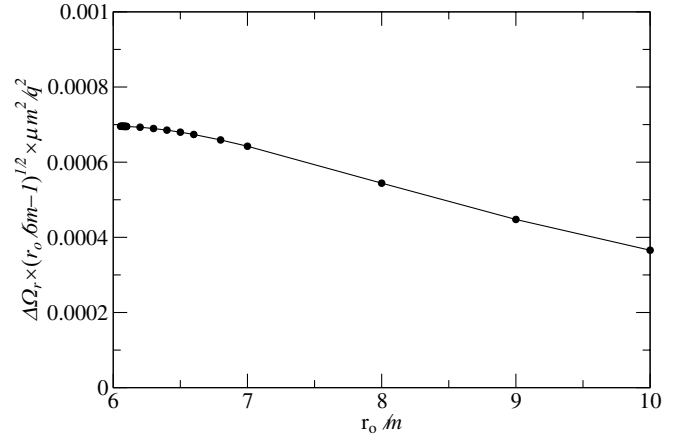


FIG. 5. For  $q^2/\mu \ll r_o - 6m$ , the change in  $\Omega_r$  from the self-force as a function of the radius  $r_o$  for slightly eccentric orbits close to the black hole. The limiting behavior at  $q^2/\mu \ll r_o - 6m \ll m$  is given in Eq. (46). See Eq. (43) for  $q^2/\mu \approx r_o - 6m$ .

#### D. Self-force effects upon $\Omega_{\text{pr}}$ for slightly eccentric orbits

The rate of precession of a slightly eccentric orbit

$$\Omega_{\text{pr}} \equiv \Omega_o - \Omega_r \quad (48)$$

is not particularly elegant when written in terms of  $m$ ,  $r_o$ , and the components of the self-force. However,

$$\Omega_{\text{pr}} = \frac{m^{1/2}}{(6m)^{3/2}} - f_0^{1/2} \quad \text{for } r_o = 6m. \quad (49)$$

In general,

$$\Delta\Omega_{\text{pr}} = \Delta\Omega_o - \Delta\Omega_r, \quad (50)$$

where  $\Delta\Omega_o$  and  $\Delta\Omega_r$  may be obtained from Eqs. (26) and (44).

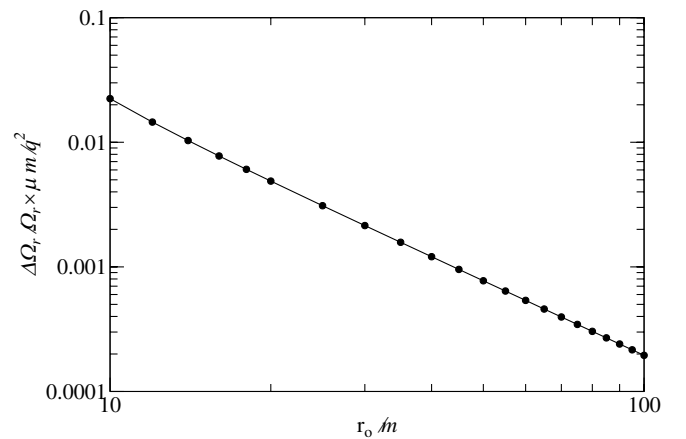


FIG. 6. From numerical analysis, the fractional change in  $\Omega_r$  from the self-force as a function of the radius  $r_o$  for slightly eccentric orbits far from the black hole.

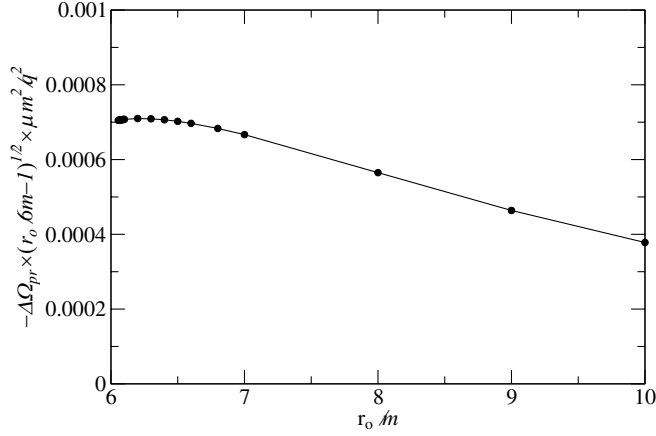


FIG. 7. For  $q/m \ll r_0 - 6m$ , the change in  $\Omega_{\text{pr}}$ , from the self-force as a function of the radius  $r_0$  for slightly eccentric orbits close to the black hole.

Figure 7 illustrates  $\Delta\Omega_{\text{pr}}$  for orbits for smaller values of  $r_0$ , and the curve for  $\Delta\Omega_{\text{pr}}$  has the same limit as that of  $-\Delta\Omega_r$  in Fig. 5. The fractional change  $\Delta\Omega_{\text{pr}}/\Omega_{\text{pr}}$  from the self-force is shown in Fig. 8 for larger values of  $r_0$  where  $\Delta\Omega_{\text{pr}}/\Omega_{\text{pr}}$  scales as  $r_0^{-1}$ .

We summarize the falloff at large  $r_0$  for a variety of quantities in Table II.

Our earlier manuscript [19] described the numerical evaluation of  $\partial_r \psi_0^{\text{R}}$  for a circular orbit in great detail. The analytically known regularization parameters (the multipole moments of  $\partial_r \psi^{\text{S}}$ ) were subtracted from the numerically determined  $\partial_r \psi_0^{\ell m}$ . A few additional regularization parameters were determined numerically and also subtracted from  $\partial_r \psi_0^{\ell m}$ . The remainder was summed over  $\ell$  up to about 40.

The main difficulty revolved around the evaluation of  $\partial_r \psi_0^{\ell m}$  with sufficient accuracy that the final sum gave us good precision. Starting with approximately 13 significant

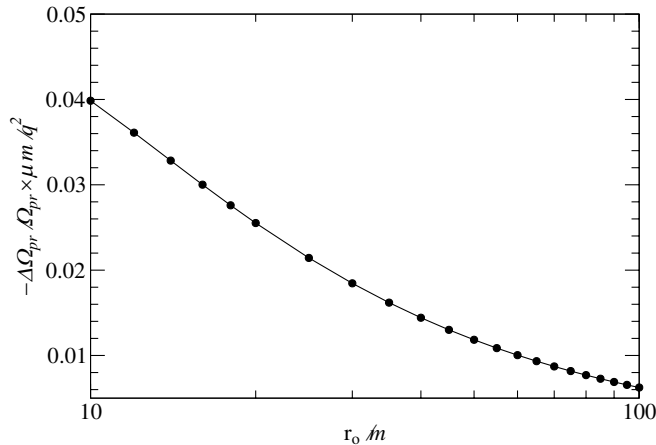


FIG. 8. For  $q/m \ll r_0 - 6m$ , the fractional change in  $\Omega_{\text{pr}}$  from the self-force as a function of the radius  $r_0$  for slightly eccentric orbits far from the black hole.

TABLE II. Falloff at large  $r_0$  for a variety of interesting quantities involving the scalar field self-force.

Quantity	behavior
$\psi_0^{\text{R}}$	$\sim r_0^{-3}$
$\partial_r \psi_0^{\text{R}}$	$\sim r_0^{-5}$
$\Omega_0$	$\sim r_0^{-3/2}$
$\Delta\Omega_0$	$\sim r_0^{-9/2}$
$\Omega_r$	$\sim r_0^{-3/2}$
$\Delta\Omega_r$	$\sim r_0^{-7/2}$
$\Omega_{\text{pr}}$	$\sim r_0^{-5/2}$
$\Delta\Omega_{\text{pr}}$	$\sim r_0^{-7/2}$
$E$	$\sim r_0^0$
$\Delta E$	$\sim r_0^{-4}$
$J$	$\sim r_0^{1/2}$
$\Delta J$	$\sim r_0^{-5/2}$

digits for  $\partial_r \psi_0^{\ell m}$ , after the regularization parameters were subtracted about eight significant digits remained. The main numerical task for evaluating the scalar field self-force effects on  $\Omega_r$  and  $\Omega_{\text{pr}}$  is very similar to this earlier work. A significant difference, however, is the need to compute  $F_t$ ,  $F_\phi$ , and  $F_r$ , introduced in Eqs. (33)–(35). The details required for determining the part of the field which depends upon the slight eccentricity of the orbit are described in Appendix A, and the regularization parameters are given in Appendix B.

## VI. SELF-FORCE EFFECT ON THE ISCO

The innermost stable circular orbit is characterized as that orbit for which  $\Omega_r$  is zero. The self-force changes the radius of the ISCO from  $6m$  by  $\Delta R$  where

$$\begin{aligned} \Delta R_{\text{is}} &\equiv (R_{\text{is}} - 6m) \\ &= 180m^2 \partial_r \psi_0 + (3/2)dJ^2/dR + 432m^3 F_r. \end{aligned} \quad (51)$$

This result follows from equating the coefficient in square brackets in Eq. (39) to zero, replacing  $r_0$  by  $6m$  in all terms which are  $O(q^2/\mu m)$  and solving for  $(r_0 - 6m)$ . The self-force correction to the angular frequency of the ISCO is given by Eq. (23) when evaluated at  $r_0 = 6m + \Delta R_{\text{is}}$ ,

$$\begin{aligned} \Omega_{\text{is}}^2 &= r_0^{-4} m (r_0 - 3\Delta R_{\text{is}}) - r_0^{-2} (r_0 - 3m) \partial_r \psi_0 \\ &= m(6m)^{-3} - 3m\Delta R_{\text{is}}(6m)^{-4} - (12m)^{-1} \partial_r \psi_0. \end{aligned} \quad (52)$$

The fractional change in  $\Omega_{\text{is}}$  from the scalar field self-force is

$$\Delta\Omega_{\text{is}}/\Omega_{\text{is}} = -\Delta R_{\text{is}}/4m - 9m\partial_r \psi_0. \quad (53)$$

A summary of our numerical results for the effect of the scalar field self-force on the ISCO is given in Table III. Our numerical work primarily followed that for evaluating  $\Omega_{\text{pr}}$ .

TABLE III. Quantities of interest regarding the ISCO.

$\Delta R_{\text{is}} \times \mu/q^2$	- 0.122 701
$\Delta \Omega_{\text{is}}/\Omega_{\text{is}} \times \mu m/q^2$	0.029 165 7

However, one subtlety involved the need for evaluating both  $F_t$  and  $F_\phi$  in the limit that  $r \rightarrow 6m$ . For that task we found each quantity at approximately 30 points between  $r = 6m$  and  $7m$ . A polynomial fit to these data, using a variety of subsets of the 30 points and different numbers of polynomial coefficients, provided robust results for the required limits.

## VII. DISCUSSION

Two parts of our analysis of the self-force effects on slightly eccentric orbits are algebraically taxing while not particularly difficult conceptually. These are the calculations of the regularization parameters and the matching of the homogeneous solutions of the field equation across the orbit of the particle. While these two steps are individually challenging, our confidence in the ultimate results is bolstered by the appropriate convergence of the sum over the  $\ell m$  modes of the components of the self-force. An error in either the analytical or the numerical work involving either the matching or the regularization parameters would be immediately heralded by a lack of convergence of the sum over modes. Consequently, we deem these results trustworthy.

We see that the effect of the self-force from a scalar field on the innermost stable circular orbit of the Schwarzschild geometry is to move the ISCO inward and to increase its angular frequency. It is tempting to generalize this result to the gravitational self-force case. But we will not do so. There is a significant difference between the self-force effects of a scalar and a gravitational field. In particular, as we mentioned in the introduction, for gravity the self-force already has an important effect at the Newtonian level [4]. Namely it is responsible for ensuring that the particle and the black hole both orbit their common center of mass. This is not the case for the scalar field. The difference may be traced back to the fact that a black hole has no scalar charge. The charged particle responds only to the gravitational interaction with the black hole and the scalar field interaction with its own  $\psi^R$ , and the particle motion deviates from a geodesic of the Schwarzschild geometry only because of its scalar field. In this limit, the black hole is not affected at all and remains fixed in space. And the particle orbit is centered upon the black hole, not upon the common center of mass. To see the motion about the center of mass, it is necessary to consider the gravitational self-force problem which we will return to in a later paper in this series.

A well-defined formulation of the stability of the ISCO requires the imposition of equal amounts of outgoing and

ingoing radiation at the boundaries to make the system dissipation-free. However, actual slow inspiral into a black hole has only outgoing radiation, and one might wonder about the relevance of our calculation to the actual physical system. Ori and Thorne [29] outline a careful treatment of the actual slow evolution of a small object inspiraling and making the transition to a plunge into a black hole. They also indicate how self-force effects could be included in their analysis. An extension of our results in the manner outlined by them is beyond the scope of this manuscript, but may be returned to in the future.

## ACKNOWLEDGMENTS

Portions of this work were discussed at the sixth Capra meeting held in June of 2003 at the Yukawa Institute for Theoretical Physics in Kyoto, Japan, with additional support from Monbukagaku-sho Grants-in-Aid for Scientific Research No. 14047212 and No. 14047214. We thank the organizers (Norichika Sago, Misao Sasaki, Hideyuki Tagoshi, Takahiro Tanaka, Hiroyuki Nakano, and Takashi Nakamura) for their hospitality during this meeting. Portions of this work were further discussed at the seventh Capra meeting held in June of 2004 at the Center for Gravitational Wave Astronomy, University of Texas, Brownsville. We thank the Center and Carlos Lousto for hospitality during this meeting. The participants of all of the recent Capra meetings have provided many fruitful discussions. This work was supported by the National Science Foundation under Grant No. PHY-0245024 with the University of Florida and under Grant No. PHY-0200852 with the University of Wisconsin-Milwaukee.

## APPENDIX A: SOURCE DECOMPOSITION FOR NEARLY CIRCULAR ORBITS

In this appendix  $m$  refers to the spherical harmonic index while  $M$  refers to the mass of the black hole. Elsewhere in this manuscript  $m$  is used for both of these quantities without confusion.

The effects of the self-force on  $\Omega_r$  and on the ISCO are governed by the scalar field  $\psi$  for a slightly eccentric geodesic. Finding the field in this case is more difficult than for a circular orbit. Apostolatos, *et al.* [28], consider the stress energy for a point mass moving along such a geodesic, in their Sections IV B and IV C, and provide an expansion of the source in powers of a small constant  $\delta R$ . Their analysis is easily modified for a scalar charge.

A slightly eccentric geodesic in the equatorial plane is described by

$$R(t) = r_o + \delta R \cos(\Omega_r t) \quad (\text{A1})$$

and

$$\Phi(t) = \Omega_o t + \delta \Phi(t) = \Omega_o t + \frac{d\Omega_\phi}{dR} \frac{\delta R}{\Omega_r} \sin(\Omega_r t), \quad (\text{A2})$$

where the angular frequency of the orbit is

$$\Omega_\phi \equiv \frac{d\phi}{dt} = \Omega_o + \frac{d\Omega_\phi}{dR} \delta R \cos(\Omega_r t). \quad (\text{A3})$$

The frequencies  $\Omega_o$  and  $\Omega_r$  are given in Eqs. (4) and (5). The quantity  $d\Omega_\phi/dR$  represents the change in angular frequency with respect to a change in radius

$$\frac{d\Omega_\phi}{dR} = -\frac{2(r_o - 3M)}{r_o(r_o - 2M)} \Omega_\phi, \quad (\text{A4})$$

while the conserved quantities  $E$  and  $J$  are held constant at their circular orbit values,

$$E^2 = \frac{(r_o - 2m)^2}{r_o(r_o - 3m)} \quad J^2 = \frac{mr_o^2}{r_o - 3m}. \quad (\text{A5})$$

The scalar field source which moves on such an orbit is

$$\begin{aligned} \varrho &= q \int_{-\infty}^{\infty} (-g)^{-1/2} \delta[r - R(s)] \delta[\phi - \Phi(s)] \delta(\theta - \pi/2) \\ &\quad \times \delta[t - T(s)] ds \\ &= \frac{q}{r^2} \left( \frac{dt}{ds} \right)^{-1} \delta[r - r_o - \delta R \cos(\Omega_r t)] \delta\left[\phi - \Omega_o t \right. \\ &\quad \left. - \frac{d\Omega_\phi}{dR} \frac{\delta R}{\Omega_r} \sin(\Omega_r t) \right] \delta(\theta - \pi/2), \end{aligned} \quad (\text{A6})$$

after an integration over  $s$  and substitutions from Eqs. (A1) and (A2). An expansion of the delta functions about the orbit, with  $\delta R$  being small, along with a spherical harmonic decomposition of this source, which includes an integration by parts over the angle  $\phi$ , yields

$$\begin{aligned} \varrho_{\ell m}(t, r) &= \oint \varrho Y_{\ell m}^*(\theta, \phi) d\Omega \\ &= \frac{q(r_o - 2M)}{r_o^3 E} Y_{\ell m}^*(\pi/2, 0) e^{-im\Omega_\phi t} \left[ 1 \right. \\ &\quad \left. - im \frac{d\Omega_\phi}{dR} \frac{\delta R}{\Omega_r} \sin(\Omega_r t) \right] [\delta(r - r_o) \\ &\quad - \delta R \cos(\Omega_r t) \delta'(r - r_o)]. \end{aligned} \quad (\text{A7})$$

This reveals that the source has a frequency spectrum consisting of the harmonics of the angular frequency  $\omega_m \equiv m\Omega_o$  along with sidebands at frequencies  $\omega_m^\pm \equiv \omega_m \pm \Omega_r$ . The amplitude of the sidebands are proportional to  $\delta R$ .

The scalar field wave equation is

$$\nabla^2 \Psi = -4\pi \varrho. \quad (\text{A8})$$

The separation of variables of  $\Psi$  yields

$$\Psi = \sum_{\ell m} \Psi_{\ell m}(t, r, \theta, \phi) = \sum_{\ell m \omega} \Psi_{\ell m}^\omega(r) e^{-i\omega t} Y_{\ell m}(\theta, \phi), \quad (\text{A9})$$

where  $\ell = 0 \dots \infty$ ,  $m = -\ell \dots \ell$ , and  $\omega = \{\omega_m, \omega_m^-, \omega_m^+\}$ . The radial equation for the  $r$  dependence of any  $\ell$  mode

with a frequency  $\omega$  is

$$\begin{aligned} \frac{d^2 \Psi_{\ell m}^\omega(r)}{dr^2} + \frac{2(r - M)}{r(r - 2M)} \frac{d\Psi_{\ell m}^\omega(r)}{dr} + \\ \left[ \frac{\omega^2 r^2}{(r - 2M)^2} - \frac{\ell(\ell + 1)}{r(r - 2M)} \right] \Psi_{\ell m}^\omega(r) = -\frac{4\pi \varrho_{\ell m}^\omega}{1 - 2M/r}. \end{aligned} \quad (\text{A10})$$

For self-force calculations it is convenient to use  $\psi \equiv (q/\mu)\Psi$  and to divide each  $\psi_{\ell m}$  into the  $\omega_m$  part  $\psi_{\ell m}^o$  and the side band parts  $\delta R \chi_{\ell m}^\pm$ ,

$$\begin{aligned} \psi_{\ell m}(t, r, \theta, \phi) &= (\psi_{\ell m}^o e^{-i\omega_m t} + \delta R \chi_{\ell m}^- e^{-i\omega_m^- t} \\ &\quad + \delta R \chi_{\ell m}^+ e^{-i\omega_m^+ t}) Y_{\ell m}(\theta, \phi). \end{aligned} \quad (\text{A11})$$

The numerical determination of these parts of  $\psi_{\ell m}$  requires the source-free solutions of Eq. (A10) with appropriate boundary conditions, and then the proper match of these solutions across the orbit of the particle at  $r_o$ . The matching conditions, from Eqs. (A7) and (A10), are

$$[\psi_{\ell m}^o]_{r_o} \equiv \lim_{\epsilon \rightarrow 0^+} [\psi_{\ell m}^o(r_o + \epsilon) - \psi_{\ell m}^o(r_o - \epsilon)] = 0 \quad (\text{A12})$$

$$\left[ \frac{d\psi_{\ell m}^o}{dr} \right]_{r_o} = -\frac{4\pi q^2}{\mu r_o^2 E} Y_{\ell m}^*(\pi/2, 0) \quad (\text{A13})$$

$$[\chi_{\ell m}^\pm]_{r_o} = \frac{2\pi q^2}{\mu r_o^2 E} Y_{\ell m}^*(\pi/2, 0) \quad (\text{A14})$$

$$\begin{aligned} \left[ \frac{d\chi_{\ell m}^\pm}{dr} \right]_{r_o} &= -\frac{4\pi q^2}{\mu r_o^2 E} Y_{\ell m}^*(\pi/2, 0) \left[ \frac{M}{r_o(r_o - 2M)} \right. \\ &\quad \left. \pm \frac{m}{2\Omega_r} \frac{d\Omega_\phi}{dR} \right] \end{aligned} \quad (\text{A15})$$

where, in the appendix only,  $[\ ]_{r_o}$  on the left-hand side denotes the discontinuous change in a quantity across the orbit at  $r_o$ .

The scalar field  $\psi$  is a purely real field, and it is convenient to combine the  $m$  and  $-m$  contributions

$$\begin{aligned} \psi_{\ell m} + \psi_{\ell, -m} &= (\psi_{\ell m}^o + \psi_{\ell m}^{o*}) \cos[m(\phi - \Omega_o t)] Y_{\ell m}(\theta, 0) \\ &\quad + (\chi_{\ell m}^+ + \chi_{\ell m}^{+*}) \delta R \cos[m(\phi - \Omega_o t) \\ &\quad - \Omega_r t] Y_{\ell m}(\theta, 0) + (\chi_{\ell m}^- \\ &\quad + \chi_{\ell m}^{-*}) \delta R \cos[m(\phi - \Omega_o t) \\ &\quad + \Omega_r t] Y_{\ell m}(\theta, 0), \end{aligned} \quad (\text{A16})$$

where we have used the fact that  $\psi$  is the conservative field given by  $\frac{1}{2}(\psi^{\text{ret}} + \psi^{\text{adv}})$ . The contribution from  $m = 0$  for a given  $\ell$  is just one-half of that in Eq. (A16) with  $m$  set to zero,

$$\begin{aligned} \psi_{\ell 0} &= \frac{1}{2}(\psi_{\ell 0}^{\circ} + \psi_{\ell 0}^{\circ*})Y_{\ell 0}(\theta, \phi) \\ &+ (\chi_{\ell 0}^+ + \chi_{\ell 0}^-)\delta R \cos(\Omega_r t)Y_{\ell 0}(\theta, \phi). \end{aligned} \quad (\text{A17})$$

Note that  $\chi_{\ell 0}^- = \chi_{\ell 0}^{+*}$  for the conservative field.

In Sec. VI we require  $\psi_{\ell m} + \psi_{\ell, -m}$  and its derivatives evaluated at the particle. The location of the particle is given in Eqs. (A1) and (A2). For  $m \neq 0$ , an expansion about  $r_o$ , retaining only terms through first order in  $\delta R$ , yields

$$\begin{aligned} (\psi_{\ell m} + \psi_{\ell, -m})_p &= \left[ 1 + \delta R(t) \frac{\partial}{\partial r} + \delta \Phi(t) \frac{\partial}{\partial \phi} \right] \\ &\times \langle (\psi_{\ell m}^{\circ} + \psi_{\ell m}^{\circ*}) \cos[m(\phi - \Omega_o t)] Y_{\ell m} \rangle \\ &+ (\chi_{\ell m}^+ + \chi_{\ell m}^{+*} + \chi_{\ell m}^- \\ &+ \chi_{\ell m}^{-*}) \delta R \cos(\Omega_r t) Y_{\ell m}, \end{aligned} \quad (\text{A18})$$

where the subscript  $p$  implies evaluation at the particle. From here through the remainder of this Appendix A, the spherical harmonic  $Y_{\ell m}$  is to be evaluated at  $(\pi/2, 0)$ , and the other terms on the right-hand sides are to be evaluated at  $(r, \phi) = (r_o, \Omega_o t)$  only after all appropriate derivatives have been taken. After simplification, this becomes

$$\begin{aligned} (\psi_{\ell m} + \psi_{\ell, -m})_p &= (\psi_{\ell m}^{\circ} + \psi_{\ell m}^{\circ*}) Y_{\ell m} + (\partial_r \psi_{\ell m}^{\circ} + \partial_r \psi_{\ell m}^{\circ*} \\ &+ \chi_{\ell m}^+ + \chi_{\ell m}^{+*} + \chi_{\ell m}^- \\ &+ \chi_{\ell m}^{-*}) \delta R \cos(\Omega_r t) Y_{\ell m}. \end{aligned} \quad (\text{A19})$$

Similar expansions start with Eq. (A16) and ultimately provide the  $\phi$  derivative

$$\begin{aligned} \frac{\partial}{\partial \phi} (\psi_{\ell m} + \psi_{\ell, -m})_p &= \left[ -\frac{m^2}{\Omega_r} \frac{d\Omega_{\phi}}{dR} (\psi_{\ell m}^{\circ} + \psi_{\ell m}^{\circ*}) \right. \\ &+ m(\chi_{\ell m}^+ + \chi_{\ell m}^{+*} - \chi_{\ell m}^- \\ &\left. - \chi_{\ell m}^{-*}) \right] \delta R \sin(\Omega_r t) Y_{\ell m}, \end{aligned} \quad (\text{A20})$$

the  $t$  derivative

$$\begin{aligned} \frac{\partial}{\partial t} (\psi_{\ell m} + \psi_{\ell, -m})_p &= \left[ \frac{m^2 \Omega_o}{\Omega_r} \frac{d\Omega_{\phi}}{dR} (\psi_{\ell m}^{\circ} + \psi_{\ell m}^{\circ*}) \right. \\ &- \omega_m^+ (\chi_{\ell m}^+ + \chi_{\ell m}^{+*}) + \omega_m^- (\chi_{\ell m}^- \\ &\left. + \chi_{\ell m}^{-*}) \right] \delta R \sin(\Omega_r t) Y_{\ell m}, \end{aligned} \quad (\text{A21})$$

and the  $r$  derivative

$$\begin{aligned} (\partial_r \psi_{\ell m} + \partial_r \psi_{\ell, -m})_p &= (\partial_r \psi_{\ell m}^{\circ} + \partial_r \psi_{\ell m}^{\circ*}) Y_{\ell m} \\ &+ (\partial_r^2 \psi_{\ell m}^{\circ} + \partial_r^2 \psi_{\ell m}^{\circ*} + \partial_r \chi_{\ell m}^+ \\ &+ \partial_r \chi_{\ell m}^{+*} + \partial_r \chi_{\ell m}^- \\ &+ \partial_r \chi_{\ell m}^{-*}) \delta R \cos(\Omega_r t) Y_{\ell m}. \end{aligned} \quad (\text{A22})$$

In Sec. VI we require the sum over  $\ell$  and  $m$  of these three previous derivatives. Accordingly, we define  $F_r$ ,  $F_{\phi}$ , and

$F_r$  from

$$(\partial_t \psi^{\text{R}})_p = -F_t \Omega_r \delta R \sin(\Omega_r t) \quad (\text{A23})$$

$$(\partial_{\phi} \psi^{\text{R}})_p = -F_{\phi} \Omega_r \delta R \sin(\Omega_r t) \quad (\text{A24})$$

and

$$(\partial_r \psi^{\text{R}})_p = (\partial_r \psi_o)_{r_o} + F_r \delta R \cos(\Omega_r t), \quad (\text{A25})$$

where the required regularization is described in Appendix B.

## APPENDIX B: REGULARIZATION PARAMETERS FOR $\psi$

We describe the regularization of the scalar field as developed by Barack and Ori [12,17] for a particle in a circular orbit of the Schwarzschild geometry. Our notation follows that of Refs. [19–21]. All of these are required reading for a thorough understanding of this appendix.

The scalar field is regularized at the location of the particle by subtracting the singular part of the field  $\psi^{\text{S}}$  from the actual field  $\psi$ . The remainder  $\psi^{\text{R}} \equiv \psi - \psi^{\text{S}}$  is then guaranteed [10] to be a regular solution of the vacuum scalar field equation in the vicinity of the particle, and the derivatives of  $\psi^{\text{R}}$  at the particle provide the required self-force resulting from the particle interacting with its own field.

The mode-sum regularization procedure [12,17] describes the multipole decomposition of  $\psi^{\text{R}}$  in terms of the decompositions of  $\psi$  and  $\psi^{\text{S}}$ ,

$$\begin{aligned} \psi^{\text{R}} &= \sum_{\ell m} \psi_{\ell m}^{\text{R}}(t, r) Y_{\ell m}(\theta, \phi) \\ &= \sum_{\ell m} [\psi_{\ell m}(t, r) - \psi_{\ell m}^{\text{S}}(t, r)] Y_{\ell m}(\theta, \phi). \end{aligned} \quad (\text{B1})$$

The numerical determination of  $\psi_{\ell m}(t, r)$  for a slightly eccentric orbit is discussed in Appendix A and in Ref. [19].  $\psi^{\text{S}}$ , however, is singular at the location of the particle, and only well defined in a neighborhood of the particle. Nevertheless, its multipole decomposition over a two-sphere of radius  $r$  is finite, even if  $r$  coincides with the radial coordinate of the particle. The decomposition is not unique because of the ambiguity in the definition of  $\psi^{\text{S}}$  away from the particle. However, the mode-sum regularization procedure remains valid because its sum is only required in a neighborhood of the particle, where the sum must equal  $\psi^{\text{S}}$ . Thus, in evaluating  $\psi^{\text{R}}$  and its derivatives at the particle the individual  $\psi_{\ell m}^{\text{S}}$  in Eq. (B1) are not unique but the sum in Eq. (B1) and its derivatives converge to unique values.

Barack and Ori [12,17] find it convenient to do the sum over  $m$  first and then to describe the multipole decomposition of a derivative of  $\psi^{\text{S}}$  as

$$(\partial_a \psi^S)_p = \sum_{\ell} \left[ \left( \ell + \frac{1}{2} \right) A_a + B_a + \frac{C_a}{\ell + \frac{1}{2}} + O(\ell^{-2}) \right], \quad (\text{B2})$$

where the  $O(\ell^{-2})$  terms yield precisely zero when summed over  $\ell$ . The constants  $A_a$ ,  $B_a$ , and  $C_a$  are independent of  $\ell$ , and are determined by a multipole decomposition of an expansion of  $\psi^S$  about the location of the particle.

The required regularization parameters for the derivatives of  $\partial_t \psi$  are derived from Eqs. (8a)–(8d) of Ref. [17]. We discuss only those parameters which have not previously appeared in an actual application [19,23]. In our notation, with  $\dot{R}$  representing a derivative of  $R$  with respect to proper time  $s$ , these regularization parameters are

$$A_{\pm t} = \pm \frac{q^2 \dot{R}}{\mu(R^2 + J^2)} \quad (\text{B3})$$

$$A_{\pm r} = \mp \frac{q^2 E}{\mu R^2 (E^2 - \dot{R}^2)} \quad (\text{B4})$$

$$A_{\pm \phi} = 0 \quad (\text{B5})$$

$$B_t = \frac{q^2 E R \dot{R}}{2\mu(R^2 + J^2)^{3/2}} (F_{1/2} - 2F_{-1/2}) \quad (\text{B6})$$

$$B_r = - \frac{q^2 R^2 [(2E^2 - \dot{R}^2)F_{1/2} - (E^2 + \dot{R}^2)F_{-1/2}]}{2\mu(R - 2M)(R^2 + J^2)^{3/2}} \quad (\text{B7})$$

$$B_{\phi} = \frac{q^2 R \dot{R} (F_{1/2} - F_{-1/2})}{2\mu J (R^2 + J^2)^{1/2}} \quad (\text{B8})$$

$$C_t = C_r = C_{\phi} = 0. \quad (\text{B9})$$

Here the hypergeometric function is represented by  $F_q \equiv {}_2F_1(q, \frac{1}{2}; 1; z)$  where the argument  $z = M/(R - 2M)$ .

These parameters may be expanded by use of Eq. (A1), which implies that

$$\dot{R} = - \frac{\delta R E \Omega_r \sin(\Omega_r t)}{1 - 2M/R}. \quad (\text{B10})$$

Through first order in  $\delta R$  the nonzero regularization parameters for a slightly eccentric orbit are

$$A_{\pm t} = \mp \frac{q^2 \Omega_r}{\mu r_o^2} \delta R \sin(\Omega_r t) \quad (\text{B11})$$

$$A_{\pm r} = \mp \frac{q^2}{\mu r_o^2 E} \left[ 1 - \frac{2}{r_o} \delta R \cos(\Omega_r t) \right] \quad (\text{B12})$$

$$B_t = - \frac{q^2 \Omega_r (F_{1/2} - 2F_{-1/2})}{2\mu r_o (r_o^2 + J^2)^{1/2}} \delta R \sin(\Omega_r t) \quad (\text{B13})$$

$$B_r = - \frac{q^2 (2F_{1/2} - F_{-1/2})}{2\mu r_o (r_o^2 + J^2)^{1/2}} \left[ 1 - \frac{2r_o^2 + J^2}{r_o (r_o^2 + J^2)} \delta R \cos(\Omega_r t) \right] + \frac{q^2 M (2F'_{1/2} - F'_{-1/2})}{2\mu r_o (r_o - 2M)^2 (r_o^2 + J^2)^{1/2}} \delta R \cos(\Omega_r t) \quad (\text{B14})$$

$$B_{\phi} = - \frac{q^2 \Omega_r (F_{1/2} - F_{-1/2})}{2\mu J (1 - 2M/r_o)^{1/2}} \delta R \sin(\Omega_r t). \quad (\text{B15})$$

In this expansion,  $F'_{1/2}$  is the derivative of the hypergeometric function  $F_{1/2}$  with respect to its argument  $z$ . Both  $F_{1/2}$  and  $F'_{1/2}$  are evaluated at  $z = M/(r_o - 2M)$ .

The regularization parameters for  $F_t$  and  $F_{\phi}$ , defined in Eqs. (A23) and (A24), are obtained by removing the factor  $-\Omega_r \delta R \sin(\Omega_r t)$  from  $A_{\pm t}$ ,  $B_r$ , and  $B_{\phi}$ . Similarly, the regularization parameters for  $F_r$ , defined in Eq. (A25), are obtained by removing the factor  $\delta R \cos(\Omega_r t)$  from the  $\delta R$  terms of  $A_{\pm r}$  and  $B_r$ .

The regularization parameters for the scalar field, alone, warrants further discussion [20]. In a particular locally-inertial coordinate system  $(T, X, Y, Z)$ , the singular field near a scalar charged particle is simply

$$\psi^S = q/\rho + O(\rho^3/\mathcal{R}^4) \quad (\text{B16})$$

where  $\mathcal{R}$  is a length scale of the geometry in the vicinity of the particle, and  $\rho^2 = X^2 + Y^2 + Z^2$ . For the special case that the particle is in a circular orbit about a Schwarzschild black hole, a coordinate transformation between the special  $(T, X, Y, Z)$  coordinates and the usual Schwarzschild coordinates allows  $\rho$  to be written as a function of Schwarzschild coordinates, and the expansion of  $1/\rho$  about  $\rho = 0$  is given in Eq. (6.22) of Messaritaki [20]. The terms of interest are

$$\frac{1}{\rho} = \epsilon^{-1} \frac{1}{\tilde{\rho}} + \epsilon^1 \left[ \frac{r_o - 3m}{8r_o^2 (r_o - 2m)} \left( \frac{1}{\chi} - \frac{(r_o + m)}{r_o} \frac{1}{\chi^2} \right) \tilde{\rho} \right] + \dots \quad (\text{B17})$$

where  $\dots$  refers to terms which vanish as  $r \rightarrow 0$  in such a manner that they have no contribution to the regularization parameters. In this equation we use

$$\tilde{\rho}^2 \equiv \frac{r_o (r - r_o)^2}{r_o - 2m} + 2r_o^2 \frac{r_o - 2m}{r_o - 3m} \chi (1 - \cos\Theta) \quad (\text{B18})$$

where

$$\chi \equiv 1 - \frac{m \sin^2 \Phi}{r_o - 2m}. \quad (\text{B19})$$

The angles  $(\Theta, \Phi)$  are derived from a rotation of the Schwarzschild coordinates which puts the particle on the  $\Theta = 0$  axis [19].

We find that, through the  $\epsilon^1$  term of Eq. (B17)

$$\psi_{\ell 0}^S(r = r_o) = B_\psi - \frac{2\sqrt{2}D_\psi}{(2\ell - 1)(2\ell + 3)} \quad (\text{B20})$$

where  $B_\psi$  and  $D_\psi$  result from the  $\epsilon^{-1}$  and  $\epsilon^1$  terms of Eq. (B17), respectively. Appendices C and D of Ref. [19] describe the expansion of the  $\Theta$  dependence in terms of Legendre polynomials and a convenient method of finding the  $m = 0$  component by integrating over the angle  $\Phi$ .

For  $\Delta = 0$ , the  $\epsilon^{-1}$  term is

$$\frac{1}{\bar{\rho}} = \sqrt{\frac{(r_o - 3m)}{2r_o^2(r_o - 2m)}} \chi^{-1/2} (1 - \cos\Theta)^{-1/2}. \quad (\text{B21})$$

From Eqs. (C3) and (D7) in [19], this gives

$$B_\psi = \sqrt{\frac{(r_o - 3m)}{2r_o^2(r_o - 2m)}} F_{1/2} \sqrt{2}. \quad (\text{B22})$$

For  $\Delta = 0$ , the  $\epsilon^1$  term is

$$\frac{1}{4} \sqrt{\frac{(r_o - 3m)}{2r_o^2(r_o - 2m)}} \left[ \frac{1}{\chi} - \frac{(r_o + m)}{r_o \chi^2} \right] \chi^{1/2} (1 - \cos\Theta)^{1/2}. \quad (\text{B23})$$

From Eqs. (C3) and (D16) in [19] this gives

$$D_\psi \frac{-2\sqrt{2}}{(2\ell - 1)(2\ell + 3)} = \frac{1}{4} \sqrt{\frac{(r_o - 3m)}{2r_o^2(r_o - 2m)}} \left[ F_{1/2} - \frac{(r_o + m)}{r_o} F_{3/2} \right] \times \frac{-2\sqrt{2}}{(2\ell - 1)(2\ell + 3)}. \quad (\text{B24})$$

- 
- [1] L. Barack and A. Ori, Phys. Rev. D **64**, 124003 (2001).  
[2] N. Sago, H. Nakano, and M. Sasaki, Phys. Rev. D **67**, 104017 (2003).  
[3] H. Nakano, N. Sago, and M. Sasaki, Phys. Rev. D **68**, 124003 (2003).  
[4] S. Detweiler and E. Poisson, Phys. Rev. D **69**, 084019 (2004).  
[5] P. A. M. Dirac, Proc. R. Soc. London A **167**, 148 (1938).  
[6] J. Jackson, *Classical Electrodynamics, Third Edition* (Wiley, New York, 1998).  
[7] B. S. DeWitt and R. W. Brehme, Ann. Phys. (Paris) **9**, 220 (1960).  
[8] Y. Mino, M. Sasaki, and T. Tanaka, Phys. Rev. D **55**, 3457 (1997).  
[9] T. C. Quinn and R. M. Wald, Phys. Rev. D **56**, 3381 (1997).  
[10] S. Detweiler and B. F. Whiting, Phys. Rev. D **67**, 024025 (2003).  
[11] E. Poisson, Living Rev. Relativity **7**, 6 (2004).  
[12] L. Barack and A. Ori, Phys. Rev. D **61**, 061502(R) (2000).  
[13] L. Barack, Phys. Rev. D **62**, 084027 (2000).  
[14] C. O. Lousto, Phys. Rev. Lett. **84**, 5251 (2000).  
[15] L. Barack and A. Ori, Phys. Rev. D **66**, 084022 (2002).  
[16] L. Barack and A. Ori, Phys. Rev. D **67**, 024029 (2003).  
[17] L. Barack, Y. Mino, H. Nakano, A. Ori, and M. Sasaki, Phys. Rev. Lett. **88**, 091101 (2002).  
[18] Y. Mino, H. Nakano, and M. Sasaki, Prog. Theor. Phys. **108**, 1039 (2002).  
[19] S. Detweiler, E. Messaritaki, and B. F. Whiting, Phys. Rev. D **67**, 104016 (2003).  
[20] E. Messaritaki, gr-qc/0308047.  
[21] D.-H. Kim, gr-qc/0402014.  
[22] L. Barack and L. M. Burko, Phys. Rev. D **62**, 084040 (2000).  
[23] L. M. Burko, Phys. Rev. Lett. **84**, 4529 (2000).  
[24] L. Barack and C. O. Lousto, Phys. Rev. D **66**, 061502(R) (2002).  
[25] Y. Mino, Phys. Rev. D **67**, 084027 (2003).  
[26] B. Carter, Phys. Rev. **174**, 1559 (1968).  
[27] C. W. Misner, K. S. Thorne, and J. A. Wheeler, *Gravitation* (Freeman, San Francisco, 1973).  
[28] T. Apostolatos, D. Kennefick, A. Ori, and E. Poisson, Phys. Rev. D **47**, 5376 (1993).  
[29] A. Ori and K. S. Thorne, Phys. Rev. D **62**, 124022 (2000).  
[30] S. Chandrasekhar and S. Detweiler, Proc. R. Soc. London A **344**, 441 (1975).  
[31] S. Detweiler, in *Sources of Gravitational Radiation*, edited by L. Smarr (Cambridge University Press, Cambridge, England, 1979), pp. 211–230.  
[32] S. Detweiler, Astrophys. J. **239**, 292 (1980).  
[33] T. C. Quinn, Phys. Rev. D **62**, 064029 (2000).  
[34] R. A. Breuer, P. L. Chrzanowski, H. G. Hughes III, and C. W. Misner, Phys. Rev. D **8**, 4309 (1973).  
[35] W. Hikida, H. Nakano, and M. Sasaki, Prog. Theor. Phys. **111**, 821 (2004).  
[36] W. Hikida, H. Nakano, and M. Sasaki, <http://arXiv.org/abs/gr-qc/0410115>.